Polymer Chemistry

Accepted Manuscript

ROYAL SOCIETY OF CHEMISTRY

www.rsc.org/polymers

Journal Name

RSCPublishing

ARTICLE

Photon Magic: Chiroptical Polarisation, Depolarisation, Inversion, Retention and Switching of Non-photochromic Light-emitting Polymer in Optofluid

Michiya Fujiki,[*,a] Yuri Donguri,[a] Yin Zhao,[b] Ayako Nakao,[a] Nozomu Suzuki,[a] Kana Yoshida[a] and Wei Zhang[*,b]

Cite this: DOI: 10.1039/x0xx00000x

Received 00th January 2012,
Accepted 00th January 2012

DOI: 10.1039/x0xx00000x

www.rsc.org/

Circularly polarized (CP)-photons at six different energies (six wavelengths) were irradiated to non-photochromic, highly photoluminescent poly[(9,9-di-*n*-octylfluoren-2,7-diyl)-*alt*-bithiophene] (**PF8T2**) as μm-sized particles in chloroform-methanol cosolvents. This approach led to the capability of photophysically controlling all chiroptical polarisation, depolarisation, inversion, retention and switching in the ground and/or photoexcited states, as proven by circular dichroism (CD), optical rotation dispersion (ORD) and circularly polarized luminescence (CPL) spectroscopy. By optofluidically tuning the refractive index of the cosolvents at 589 nm (n_D), these CP-photon induced CD signals were *resonantly enhanced* at a specific n_D of ≈ 1.40. Surprisingly, regardless of the same *l*- (and *r*-) CP hand, the choice of higher- and lower CP-photon energies led to a swapping of signs in chiroptical polarization of the particles. CP-photon hand, *l*- and *r*-, was *not a deterministic factor for the induced chiroptical sign* of the **PF8T2** particles. This anomaly originates from CD inversion characteristics between lower and higher energy regions, supported by ZINDO calculation of **PF8T2** model oligomers. Finally, controlled CP-photon sense and irradiating energy successfully allowed CPL-silent **PF8T2** particles (quantum yield of 15 %) to change to CPL-active particles on the order of $|g_{CPL}| = (1.9-4.3)\times10^{-3}$ at ≈ 535 nm whilst almost keeping the quantum yield of 8 %.

1. Introduction

In 1926, Gilbert Lewis coined the term, *photon,* meaning quantised light.[1] Although a photon is known to be a massless elemental particle (gauge boson), quantum optics tells us that left (*l*)- and right (*r*)-circularly polarized (CP)-photons convey *integer* angular momentum (spin), $+\hbar$ and $-\hbar$, respectively.[2] This pioneering work is recognised as the first CP-photon chirality transfer experiment, enabling to rotate a macroscopic quartz plate with the help of a torsion balance. Furthermore, because a photon carries orbital angular momentum,[3a] two μm-sized polymer solid particle made of non-photochromic achiral PTFE can rotate in clockwise and counterclockwise directions.[3b] This was achieved by adding and subtracting spin and orbital angular momenta of photon. Allen *et al.* named optical spanner.[3b] This idea led to the optical vortex: squeezing μm-sized droplet of non-photochromic liquid crystal in water.[3c] A series of these experiments is now recognised as photon chirality transfer to photophysically and mechanically drive achiral, non-chromic chemical substances.[3d,3e]

Integer photonic spin makes plural spins confine in an ultrasmall space with the same quantum states, while *half integer* spin (fermion), like electron, denies sharing the same quantum states in a molecular space, known as the Pauli exclusion principle.[2] Intense CP-photons act as a parity-conserving energy source that preferentially generate optically active substances from prochiral substances and/or preferentially decomposes one enantiomer from racemic mixtures.[4] In contrast, a weak CP-photon source is used to characterise chiral substances in the ground and photoexcited states, known as circular dichroism (CD), optical rotation dispersion (ORD), circularly polarized luminescence (CPL), circular differential scattering (CDS) and vibrational circular dichroism (VCD).[5]

On the other hand, knowledge and understanding of an efficient generation and switching of optically active substances with a desired chirality from achiral precursors in the absence of chiral chemical influence have long been challenging. This approach, called absolute asymmetric synthesis (AAS), is beneficial to avoid multiple-step synthesis that often require

designed catalysts and specific chiral chemical sources with high *ee*.[4] Several AASs have been employed so far, including spontaneous symmetry breaking crystallization,[6] mechanophysical stirring,[7] unpolarised and linearly polarised photon sources under magnetic field,[8] longitudinal spin-polarised electron[9] and CP-photon irradition.[10] In an analogy with the electron spin, CP-photon is regarded as longitudinal spin-polarised particles. Alternatively, a possibility of handed AAS is postulated based on greatly amplified scenario reflecting from ultra-subtle, parity-violating weak nuclear forces.[11] Recently, controlled generating and swapping *l*- and *r*-CP-light source using elaborate devices are possible by applying external electrical field to ambipolar transistor of tungsten diselenide and by metamaterial geometry of sub-μm size pattered gold film.[12]

Alternatively, *r*- or *l*-CP-photon source in γ-ray, X-ray and vacuum UV region is assumed to be one candidate for physical and astrophysical origin of biomolecular handedness on Earth and interstellar medium.[4,13] One-hand of CP-photon source should play key roles in complex biological functions by dictating invisible twisting forces; conversely, the other hand of CP-photon source may depolarise and/or invert these substances. CP-photon induced AAS experiments are regarded as photon chirality transfer to drive photochemically chirality of substances. So far, photochromic chromophores have been mainly employed.[10f-10h,10j-10n] Recent studies using CP-photon as chiral physical source demonstrated that achiral non-photochromic π□□□□□□□□□□□□□ polyfluorene, poly(1-substituted phenylacetyelene), diacetylene monomers and Cu(II) coordinated with succinate and 4,4'-bipyridine can provide the corresponding optically active polymers.[14] However, these CP-driven AAS experiments are mostly carried out at a single photon energy source because it is long assumed that product chirality is governed by solely *r*- or *l*-hand of CP-photon and is not significantly influenced by CP-photon energy.

In 1972, Calvin *et al.* reported the first CP-photon energy dependent ring-closure reaction of *cis*-1,2-diarylethyele rotamer in the presence of iodine to yield non-racemic octahelicene in toluene. A preference of the optical activity led by *l*-CP source at 290 nm was opposite to that by *l*-CP sources in the range of 310−410 nm and *vice versa*, reflecting the bisignate CD signal of octahelicene.[10c] Recently, CP-photon energy dependent photodegradation of racemic $^{[13]}$C-alanine film was reported. Preference of the product chirality in the film was inverted by CP-photon energy source. This inversion arises from bisignate CD sign characteristics in the irradiation region [6.19 eV (200 nm) or 6.74 eV (184 nm)].[13d] Similarly, we reported that CP irradiation photon dependent chiroptical inversion takes place in photochromic di-*n*-octylfluorene-azobenzene alternating copolymer (**PF8AZO**, Scheme1) when the same *r*- and *l*-CP-photon sources were applied.[10n]

An open question is whether photon chirality transfer to achiral non-photochromic colloidal particles dispersed in optofluidic medium is possible photophysically and/or photochemically under controlled conditions with reversibility. This system is a model of prebiotic evolution of non-photochromic biological polymers in heterogeneous conditions under far-from-equilibrium open system, allowing a continuous CP-photon energy flow in the daytime.[10n,15] Optically active generated substance is regarded as a dissipated structure.

To answer this question, we chose μm-sized polymer particles of poly[(9,9-di-*n*-octylfluoren-2,7-diyl)-*alt*-2,2'-bi-thiophene] (**PF8T2**, Scheme 1). Optically inactive **PF8T2** is non-photochromic but highly photoluminescent with a high quantum yield (Φ_{PL}).[16] The particles, which consist of particles ≈0.6−0.7 μm in diameter, provide ultrasmall microreactors to efficiently confine CP-photons by tuning the refractive index (RI) of chloroform/methanol ($CHCl_3$/MeOH) cosolvent that acts as an optofluidic medium.[10n,17,18] Noting that wavelength of incident light in a vacuum markedly shortens proportional to inverse RI in the particle: *i.e.* incident light (λ_0 = 500 nm in a vacuum) is roughly estimated to be 250 nm in the polymer particle, enabling confinement of photons into the 0.6−0.7 μm sized particle when the RI of the particle is assumed as 2.0 (*e.g.*, RI = 1.9 at 486 nm for **PF8AZO**[10n]). Conversely, the speed of light in the polymer slows down to half of that in a vacuum of 3.0 x 10^8 m sec^{-1}.

Herein, we report that (i) *l*- and *r*-CP-photon induce chiroptical polarization, depolarization, inversion, retention and switching to **PF8T2** particles, and that (ii) these CD signals are resonantly enhanced at a specific RI value at 589 nm (n_D) of the cosolvents. Furthermore, (iii) regardless of the same hand of CP-photon, the choice of higher- and lower-CP-photon energies swaps the CD sign of the products and (iv) molecular mass of **PF8T2** considerably affects these CD and UV-visible spectral characteristics. This sign-swapping originates from inherent chiroptical inversion characteristics of **PF8T2** and **PF8AZO**, suggested by ZINDO simulation for these hypothetical models.

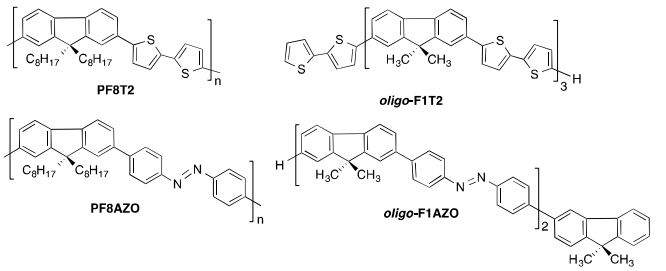

Scheme 1. Chemical structures of poly[(9,9-di-*n*-octyl-fluoren-2,7-diyl)- *alt*-bithiophene] (**PF8T2**), poly[(9,9-di-*n*-octylfluoren-2,7-diyl)-*alt*- azo-benzene (**PF8AZO**) and the corresponding model oligomers, ***oligo*- F1T2** and ***oligo*-F1AZO**.

2. Experimental Part

2.1 Materials

Spectroscopic grade $CHCl_3$ and MeOH (Dojindo, Kumamoto, Japan) were used as received. **PF8T2** was purchased from American Dye Source, Inc. (Quebec, Canada). Higher molecular mass ***h*-PF8T2** (M_w = 4.13 x 10^4, M_n = 2.45 x 10^4, M_w/M_n = 1.68) by fractional precipitation ($CHCl_3$ and MeOH) of this **PF8T2** was mainly used for measurement. For comparison, lower molecular mass ***l*-PF8T2** (M_w = 2.33 x 10^4,

M_n = 1.48 x 10^4, M_w/M_n = 1.58) was purchased from Sigma-Aldrich Japan (Tokyo, Japan) and was used as received. Appearance of ***h*-** and ***l*-PF8T2** powders were considerably different from each other. To the naked eye, the former and latter were orange and yellow colours, respectively. However, wide-angle X-ray scattering (WAXS) data of the ***h*-PF8T2** powder had *d*-spacings of 4.44 Å and 16.9 Å (ESI, Fig. S1), almost identical to that of ***l*-PF8T2**.[16a] Herein, we focused on randomly oriented **PF8T2** particles dispersed in poorer optofluidic cosolvents to avoid unfavourable alterations in chiroptical sign and magnitudes of a partly oriented **PF8T2** film.

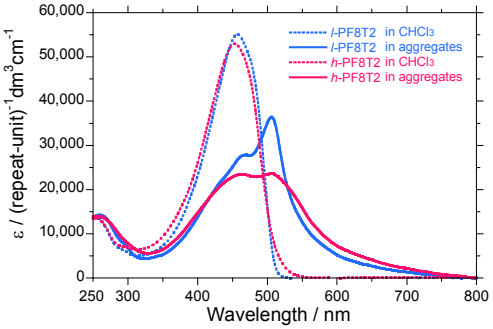

Fig. 1. A comparison of UV-visible spectra of ***h*-PF8T2** (dotted orange line) and ***l*-PF8T2** (dotted green line) in $CHCl_3$ and the corresponding particles of ***h*-PF8T2** (solid orange line) and ***l*-PF8T2** (solid green line) in MeOH/$CHCl_3$ cosolvents. The respective ***h*-** and ***l*-PF8T2** particles were prepared in MeOH/$CHCl_3$ = 1.8/1.2 (v/v) and 2.1/0.9 (v/v).

The UV-visible spectra of these particles were much different, though the difference in their dilute chloroform solutions was not evident (Fig. 1). Meanwhile, these ***h*-** and ***l*-PF8T2** particles were prepared in MeOH/$CHCl_3$ = 1.9/1.1 (v/v) and 1.8/1.2 (v/v)), respectively. Considerable differences in UV-visible spectra (two λ_{max} values at ≈455 nm and ≈505 nm, their relative absorptivity and absorption edge at longer wavelength) between ***h*-** and ***l*-PF8T2** particles can be seen. The origin of this apparent colour alteration could be ascribed to three possibilities: (i) disordered and ordered states, (ii) the existence and non-existence of intermolecular charge-transfer states and (iii) "A"-conformation (like α-phase) □□□ □"B"□conformation (like β-phase), elucidated by recent work in temperature dependent PL dynamics in solution state.[19] An alternative idea arises from more extended π-conjugation of ***h*-PF8T2** due to a longer repeating unit, compared to that of ***l*-PF8T2**.

Regardless of ***h*-** and ***l*-PF8T2** particles, a great redshift of ≈ 50 nm in the longest π–π^* transitions clearly indicated the production of *J*-particles responsible for highly photolumine-scent states.[20] Actually, the λ_{max} of ***h*-** and ***l*-PF8T2** in $CHCl_3$ is located at ≈ 455 nm, whereas that of the particles exists around 506–508 nm.

2.2 Characterisation

The CD, ORD and UV-visible spectra of the solutions were recorded on JASCO J-725 spectropolarimeters with 450-W water-cooled Xenon lamp (Osram, München, Germany) (Hachioji-Tokyo, Japan) equipped with Peltier-controlled housing and synthetic quartz (SQ) cuvettes with 1.0 cm path length (scanning rate: 200 nm min^{-1}, bandwidth: 2 nm, response time: 2 s, a single accumulation, data sampling: 0.5 nm interval) at 25 °C. UV-visible spectra were corrected to subtract an increment in background signals due to particle scattering by adjusting to be absorbance zero at 800 nm in the original UV-visible spectral data, while CD spectral data not susceptible to particle scattering were used without data processing. The CPL and photoluminescence (PL) spectra were recorded on a JASCO CPL-200 spectrofluoro-polarimeter (150-W air-cooled Xenon lamp (Osram), detected at an angle of 0° with a notch filter (1:10^6), a path length: 1.0 cm at ≈ 25 °C, a scanning rate: 200 nm min^{-1}, a slit width for excitation: 2000 μm at 400 nm, a band width for monitor: 10 nm, a response time: 2 s, data sampling: 1.0 nm interval. PL quantum yield (Φ_{PL}) of **PF8T2** particles was evaluated by a relative method using an ethanol solution (2.0 × 10^{-6} mol L^{-1}, Φ_{PL}: 90%) of fluorescein (TCI, Tokyo, Japan) as a reference. The Φ_{PL} value of ***h*-PF8T2** in homogeneous $CHCl_3$ solution was obtained with ≈60%. PL spectra were recorded on a JASCO FP-6500 spectrofluorometer (a path length: 10 mm, a band width for excitation: 5 nm, a band width for monitor: 2 nm, a response time: 2 sec, excitation: 450 nm, data sampling; 2.0 nm interval). The n_D value was estimated by the equation that $n_{D,ave}$ = x•$n_{D(MeOH)}$ + (1-x)•$n_{D(CHCl3)}$, x: volume fraction of MeOH in cosolvent. Weight-average molecular mass (M_w) and number-average molecular mass (M_n) were obtained with gel-permeation chromatography (GPC) (Shimadzu 10A) using a Plgel mixed-B (10 μm, 4.6 mm in i.d., 20 cm in length, Agilent Technology) and tetrahydrofuran as an eluent based on a calibration of polystyrene standards. Particle sizes were analysed by dynamic light scattering (DLS) (detector with 90° and accumulation: 30 times) DLS-6000, Otsuka Electronics, Hirakata-Osaka, Japan) using solution viscosity data obtained with a Sekonic (Tokyo, Japan) viscometer VM-100 at 25 °C and n_D value of MeOH and $CHCl_3$ at 589 nm at 25 °C by Atago (Tokyo, Japan) refractometer DR-M2. All data acquired by these methods were re-analysed using KaleidaGraph ver. 4.13 (Synergy software, Pennsylvania, USA). Fluorescence optical microscope (FOM) images were obtained as jpeg data with a Nikon (Tokyo, Japan) Eclipse E400 with a filter block B2A (450-490 nm for excitation with a cut filter shorter than 500 nm). HRTEM images were obtained using a JEOL (Hachioji-Tokyo, Japan) JEM-3100FEF electron microscope (accelerating voltage of 300 kV, bright-field image). WAXS data with θ–2θ scan (θ: 2–50 deg) were collected using a Rigaku (Akishima-Tokyo, Japan) R-AXIS-IV wide-angle X-ray diffractometer (Ni-filtered CuKα, 50 kV) and analysed by Rigaku built-in image processing software.

2.3 CP-photon irradiation apparatus

A home-made *l*- and *r*-CP-photon irradiation apparatus, enabling emission of several bright lines, was configured with an Ushio (Tokyo, Japan) Optiplex BA-H501 and a power

supply USH-500SC2 installed with ultrahigh pressure air-cooled 500-W mercury lamp (Ushio), six narrow band-pass filters [3.96 eV (313nm), 3.40eV (365 nm), 3.06 eV (405 nm), 2.84 eV (436 nm), 2.27 eV (546 nm) and 2.15 eV (577 nm)] supplied by Sigma Koki (Tokyo, Japan) and Asahi Spectra (Tokyo, Japan), UV-grade Glan-Taylor calcite prism (250–2300 nm, Sigma Koki) and six quartz-made quarter-wave plates (Sigma Koki) specified for these six wavelengths, as outlined in Scheme 1 of ref. 10n. The irradiation power intensity was checked with a broad range Si photodetector (Nova PD300-UV, Ophir-Japan (Tokyo, Japan)), as given in ESI, Table S1†.

2.4 Preparation of PF8T2 particles

PF8T2 particles in a mixed $CHCl_3$ and MeOH cosolvent were produced by aggregation process. A typical procedure was as follows. First, 1.5 mL of methanol was added dropwise (typically, one drop of methanol per sec using a micropipette) to 1.5 mL of a $CHCl_3$ solution containing **PF8T2** to tune a final concentration ($[\text{repeat unit}]_0 = 3.5 \times 10^{-5}$ mol L^{-1}) in the SQ cuvette at room temperature, under a mild stirring for 20 sec to prevent mechanophysical induced chiroptical effects. This handheld operation allowed us to produce yellowish, turbid **PF8T2** particles, followed by CP-photon irradiation experiments. Although our previous work showed that optically active ***l*-PF8T2** particles are instantly generated by limonene chirality transfer,[16] CP-photon induced experiments of ***l*-PF8T2** particles have not been reported.

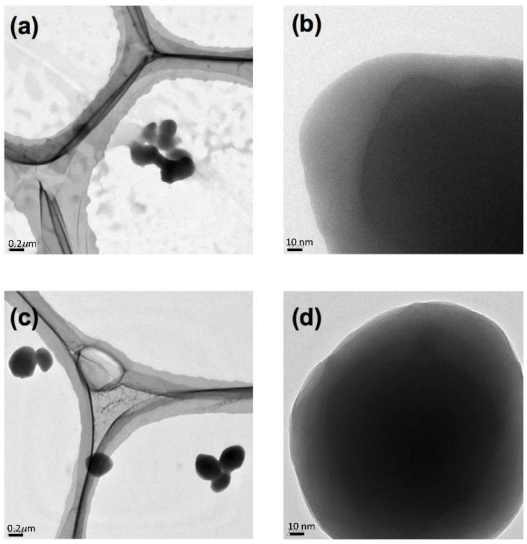

Fig. 2. HRTEM images of ***h*-PF8T2** particle (a and b) before irradiating and (c and d) after *r*-CP-photon at 546 nm for 60 min. Scale bar: 0.2 μm (a and c) and 10 ⍰m (b and d).

The size of the **PF8T2** particles in $CHCl_3$/MeOH (2.1/0.9 (v/v)) cosolvent, before and after irradiation with *r*-CP-photon at 546 nm for 30 min, were characterised by DLS measurement to be typically 0.91 μm in diameter and 0.55 μm in diameter (ESI, Figs. S2(a)-(c), Table S2). However, the actual size and shape are obscure due to the blurring effect. Additional HRTEM images suggested that the CD-active and CD-silent ***h*-PF8T2** particles are typically ~500 nm in diameter (Figs. 2a and 2b, and ESI, Fig. S3(a)) and ~600 nm (Figs. 2c and 2d, and ESI, Fig. S3(b)), respectively. Those particles, though dried, adopted a slightly irregular, sphere-like shape, possibly, that could be used as a photon-induced microreactor.

2.5 Gaussian03 ZINDO calculation of *oligo*-F1T2 and *oligo*-F1AZO as models of PF8T2 and PF8AZO

All calculations were carried out using Gaussian03 (rev. E)[21] running on an Apple PowerMac (dual QuadCore, 2.8 GHz, 32GB memory, MacOS ver.10.5.8, 2TB hard disk). The most probable structures of ***oligo*-F1T2** and ***oligo*-F1AZO** (Scheme 1) in the ground state were optimised using MM-UFF, followed by PM3 calculations. Simulated UV-visible and CD spectra of ***oligo*-F1T2** and ***oligo*-F1AZO** were obtained with semi-empirical ZINDO with forty or twenty transition states.

3. Results and Discussion

3.1 CP-photon energy dependence of chiroptical polarization

No chiroptical polarization of ***h*-PF8T2** dissolved in $CHCl_3$ before CP-photon irradiation and after *r*-CP-photon irradiation at 546-nm was confirmed, though faint chiroptical polarization ($|g_{CD}| \approx$ (1–2) x 10^{-5} at 480 nm) of ***h*-** and ***l*-PF8T2** in homogeneous $CHCl_3$ solution by prolonged irradiation of *l*- and *r*-CP-photon can be seen (ESI, Fig. S4).

Figs. 3a–3b show the CD and UV-visible spectra of ***h*-PF8T2** particles in $CHCl_3$/MeOH (2.1/0.9 (v/v)). Fig. 3c–d shows ***l*-PF8T2** particles in $CHCl_3$/MeOH (1.8/1.2 (v/v)). These CD and UV-visible spectra were induced by irradiating six different wavelengths of *l*- and *r*-CP-photon for 60 min. Noting that no detectable CD signals in non-irradiated **PF8T2** particles in these media are observed because these particles are originally CD-silent and/or achiral states. No chiroptical polarization of the particles happens during the aggregation process.

However, it is evident that these induced CD bands are inverted by the choice of longer and shorter wavelengths as irradiation energy. The changes in g_{CD} values of ***h*-PF8T2** particles in $CHCl_3$/MeOH (2.1/0.9 (v/v)) are plotted as a function of irradiation time (0–120 min) of *l*- and *r*-CP-photons at six wavelengths (Figs. 3a–3d and Fig. S5 (ESI)).

From Figs. 3a–3b, when the ***h*-PF8T2** was irradiated at 546 nm and 577 nm by *r*-CP-photon, a positive CD band at 536 nm and negative CD band at 386 nm appeared newly, while, by *l*-CP-photon, these signs were inverted. Conversely, when the ***h*-PF8T2** was irradiated at 313 nm and 365 nm by *r*-CP-photon, a negative CD band at ≈ 535 nm and positive CD band at ≈ 390 nm appeared, while, these signs by *l*-CP-photon were inverted.

On the other hand, from Figs. 3c–3d, the ***l*-PF8T2** irradiated at 436 nm and 546 nm by *r*-CP-photon revealed a positive CD band at ≈ 515 nm and a negative CD band at ≈ 375 nm appeared, while, when by *l*-CP-photon, these signs were definitively inverted. Conversely, the ***l*-PF8T2** irradiated at 313 nm and 365 nm by *r*-CP-photon provided a negative CD band

at ≈ 525 nm and a positive CD band at ≈ 385 nm appeared, while *l*-CP-photon showed these mirror-image CD profiles.

The λ_{ext} values at the first Cotton CD bands depended slightly on ***h*-** and ***l*-PF8T2** that the former and latter are located at ≈ 535 nm and ≈ 525 nm, respectively. More notably, the first Cotton CD band of ***h*-PF8T2** is efficiently induced by the 546-nm irradiation, while, that of ***l*-PF8T2** is easily induced by the 436-nm irradiation. These differences arise from the considerable differences in UV-visible spectra between ***h*-** and ***l*-PF8T2** particles and subtle differences in solution state UV-visible spectra between ***h*-** and ***l*-PF8T2**, as seen in Fig. 1.

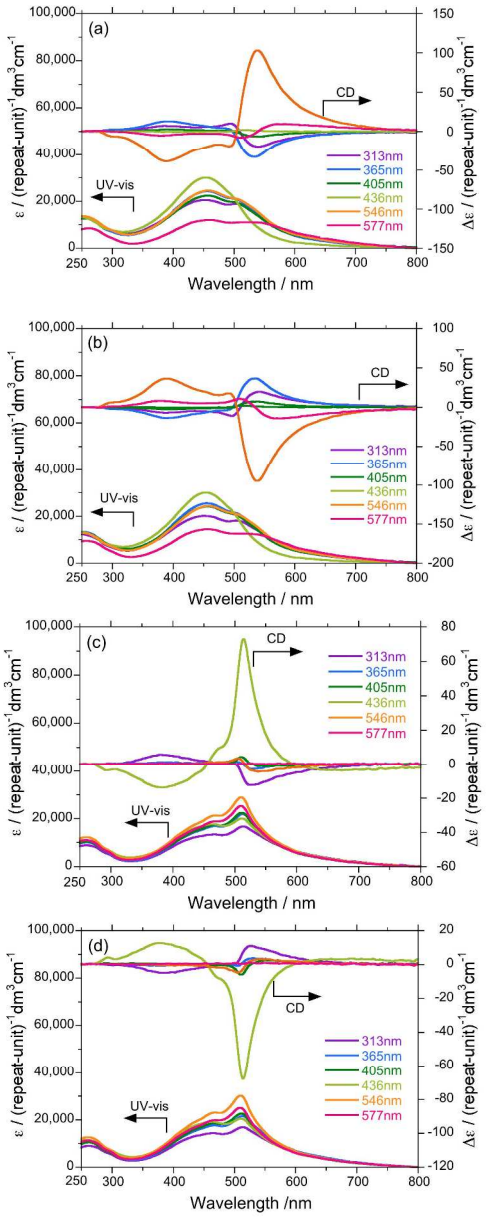

Fig. 3. CD and UV-visible spectra of ***h*-** and ***l*-PF8T2** in $CHCl_3$/MeOH cosolvents induced by *r*- and *l*-CP-photon at six different photon energies for 60 min. ***h*-PF8T2** in $CHCl_3$/MeOH (2.1/0.9 (v/v)) and ***l*-PF8T2** in $CHCl_3$/MeOH (1.8/1.2 (v/v)), respectively. (a) ***h*-PF8T2** with *r*-CP-photon, (b) ***h*-PF8T2** with *l*-CP-photon, (c) ***l*-PF8T2** with *r*-CP-photon, (d) ***l*-PF8T2** with *l*-CP-photon.

Noted that, particularly, CD and UV-visible spectroscopic properties of ***h*-PF8T2** strongly depend on the CP-photon irradiation wavelengths (Fig. 3(a)(b)). We assume that significant alterations in the wavelength shifts and UV-visible/CD spectral shapes are ascribed to the "A-B" transition, order-disordered transition and/or production of plural rotational isomers in the particles.[19]

3.2 Refractive index dependence of optofluidic medium

The cosolvent ratios shown above were optimised by optofluidically tuning the refractive index (n_D) of the cosolvents because those CP-photon induced CD signals were resonantly enhanced at a very specific n_D of ≈1.40, as given in Fig. 4 as filled circles for ***h*-PF8T2** and squares for ***l*-PF8T2**, respectively. For comparison, chiroptical polarization of ***l*-PF8T2** particles induced by limonene chirality transfer in (*R*)-limonene (**1*R***)/$CHCl_3$/MeOH (2.0/0.3/0.7 (v/v/v)) tersolvents, in which the original data taken from a previous study were re-edited as an n_D value. It is worth noting that the g_{CD}-n_D relationships are very narrow distribution for CP-photon induced ***h*-** and ***l*-PF8T2** particles, while rather broader distribution for **1*R*** induced ***l*-PF8T2** particles, because the CP-photon particles adopt the spherical-like shapes, while the **1*R***-induced particles have very irregular shapes with a jagged surface.[16a] An ideally spherical shape with a smooth surface satisfies a very narrow resonance condition, which is one of major benefits of constructing an ideal optofluidic system.[17]

The g_{CD} values of **PF8T2** particles are resonantly magnified at different n_D values of the cosolvent. The g_{CD} value of ***l*-PF8T2** is enhanced at n_D =1.395, while that of ***h*-PF8T2** is enhanced at a higher n_D =1.412. This tendency might be connected to the fact that the λ_{ext} value of ***h*-PF8T2** particles is longer than that of ***l*-PF8T2** particles, implicating that the refractive index of ***h*-PF8T2** particles is slightly higher than that of ***l*-PF8T2** particles.

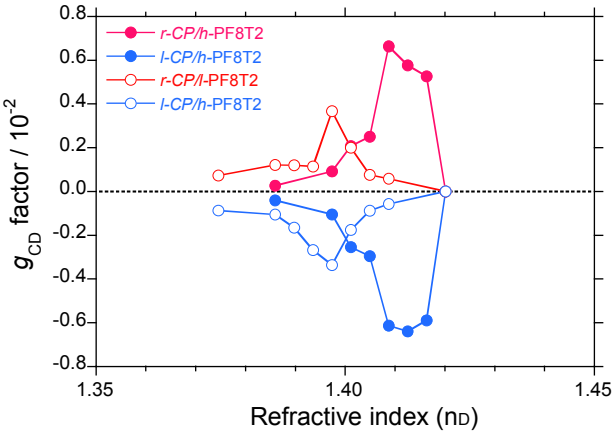

Fig. 4. The g_{CD} factors of ***h*-** and ***l*-PF8T2** in $CHCl_3$/MeOH cosolvents as a function of refractive index (n_D) at 589 nm of $CHCl_3$/MeOH cosolvent. Red and blue filled circles show chiroptical polarization of ***h*-PF8T2** particles induced by *r*- and *l*-CP-photons at 2.27 eV (546 nm) for 60 min irradiation, respectively, meanwhile, red and blue open circles are those of ***l*-PF8T2** induced by *r*- and *l*-CP-photons at 2.84 eV (436 nm) for 60 min irradiation, respectively.

However, regardless of CP-photon induced and (*R*)-limonene-induced chiroptical polarization, CD amplitude resonantly maximised at n_D value of ≈1.40±0.05. The CD amplitude decreases above and below the n_D value. This feature is evidence of an optofluidic effect due to confinement of CP-photon in the particles with the help of the surrounding organic cosolvent. Similar effects are already reported in several limonene-induced optically active π- and σ-conjugated polymer particles,[17h,17i] as well as CP-photon induced optically active π-conjugated polymer.[10n] These specific RI values of the surrounding solvents relative to the higher RI value of π-conjugated **PF8T2** partly fulfils an attenuated resonant condition of imperfect cavity in terms of whispering gallery mode (WGM) of an ideal spherical microresonator.[22]

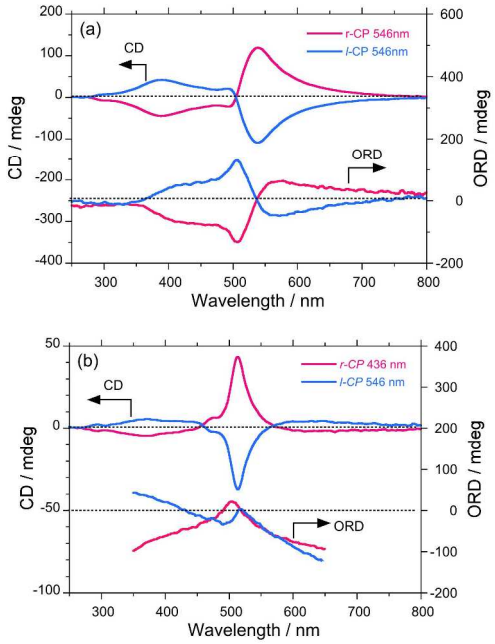

Fig. 5. (a) The CD and ORD spectra of ***h*-PF8T2** and ***l*-PF8T2** in $CHCl_3$/MeOH cosolvents. Chiroptical polarization of *h*-PF8T2 particles is induced by *r*- and *l*-CP-photons at 2.27 eV (546 nm) for 60 min irradiation, respectively, (b) those of ***l*-PF8T2** induced by *r*- and *l*-CP-photons at 2.84 eV (436 nm) for 60 min irradiation, respectively. The maximised g_{CD} values of ***h*-** and ***l*-PF8T2** in the optimised cosolvent induced by *r*- and *l*-CP-photons for 60 min: ***h*-PF8T2** in $CHCl_3$/MeOH (2.1/0.9 (v/v)) at 2.27 eV (546 nm), ***l*-PF8T2** in $CHCl_3$/MeOH (1.8/1.2 (v/v)) at 2.84 eV (436 nm), respectively.

3.3 Comparison of CD and ORD spectra between *h*- and *l*-PF8T2 particles

To elucidate several factors responsible for CP-photon induced chiroptical polarization, we measured ORD spectra of ***h*-** and ***l*-PF8T2** particles to compare the corresponding CD spectra, as given in Fig. 5. The ORD spectra reflects the difference in refractive index connecting to light speed between *l*- and *r*-CP-photon when *l*- and *r*-CP-photons travel within the particles, while CD spectra directly connect the difference in absorbance between *l*- and *r*-CP-photon within the particle.

Although ORD and CD spectra of ***h*-PF8T2** particles are ideal mirror image relationships, respectively (Fig. 5(a)), zero-dispersion wavelengths in ORD and CD spectra are different; 536 nm for ORD; 506 nm for CD spectra. The wavelength of 536 nm in ORD spectra indicates no differences in refractive index and light speed between *l*- and *r*-CP-photons. The wavelength of 506 nm in CD spectra indicates no differences in absorptivity between *l*- and *r*-CP-photon.

It is noting that, although CD spectra of ***l*-PF8T2** particles are in ideal mirror image relationships, CD spectral shapes with λ_{ext} values between ***h*-** and ***l*-PF8T2** particles are greatly different, reflecting from considerable differences in UV-visible spectral shape of ***h*-** and ***l*-PF8T2** particles (Fig. 1). zero-Dispersion wavelengths in CD spectra are 457 nm and ORD spectra of ***l*-PF8T2** particles, though are distorted due to unresolved reason, zero-dispersion wavelength may be 467 nm (Fig. 5(b)).

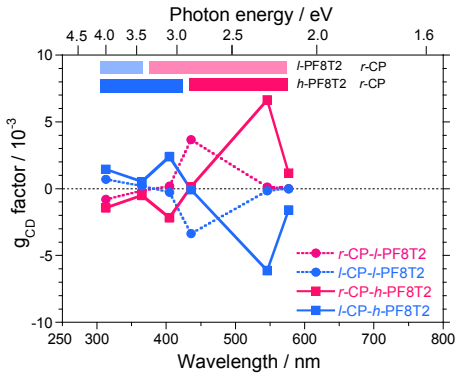

Fig. 6. The irradiation wavelength (and photon energy) dependent g_{CD} values of ***h*-** and ***l*-PF8T2** in the optimised cosolvent conditions induced by *r*- and *l*-CP-photons for 60 min: ***h*-PF8T2** in $CHCl_3$/MeOH (2.1/0.9 (v/v)) at 2.27 eV (546 nm), ***l*-PF8T2** in $CHCl_3$/MeOH (1.8/1.2 (v/v)) at 2.84 eV (436 nm), respectively.

For visibility, the irradiation wavelength (and photon energy) dependent g_{CD} values of ***h*-** and ***l*-PF8T2** particles in the optimised cosolvent induced by *r*- and *l*-CP-photons for 60 min are charted in Fig. 6. For the ***h*-PF8T2** particle, chiroptical CD signals irradiated at 546 nm are rather efficient at 577 nm, and inefficient at 436 nm. The $|g_{CD}|$ factor maximises at 546 nm and weakens at 463 nm. The difference in absorbance between *l*- and *r*-CP-photon (CD mode) is a more important factor than the difference in light speed (ORD mode) between *l*- and *r*-CP-photon. On the other hand, for the ***l*-PF8T2** particle, chiroptical CD signals irradiated at 436 nm are efficient compared to those at 405 nm and 546 nm, and inefficient at 577 nm. The $|g_{CD}|$ factor at 436 nm is weaker than that of 546 nm.

Swapping of signs in chiroptical polarization induced by the same *l*- and *r*-CP-photons is likely to occur at ≈ 436 nm for ***h*-PF8T2** particles and ≈ 405 nm for ***l*-PF8T2** particles, respectively. These swapping wavelengths, however, are inconsistent with the zero-dispersion wavelengths in ORD (536 nm, 467 nm) and CD (506 nm, 457 nm) spectra. A possible reasoning for this will be discussed in section 3.7.

3.4 CP-photon induced CPL-active PF8T2 particles

Fig. 7 compares CPL and PL spectra of (a) ***h*-PF8T2** particles after *r*- and *l*-CP-photon irradiation at 546 nm for 60 min and

(b) ***l*-PF8T2** particles prepared by the limonene chirality transfer using [(*R*)- and (*S*)-limonene]/$CHCl_3$/MeOH (2.0/0.3/0.7 (v/v)) tersolvent. For CP-photon induced ***h*-PF8T2** particles, the magnitudes of CPL, defined as g_{CPL}, are –1.1 x 10^{-3} at 494 nm, +1.6 x 10^{-3} at 530 nm and –3.6 x 10^{-3} at 530 nm for *l*-CP, while, –1.1 x 10^{-3} at 494 nm, –2.7 x 10^{-3} at 530 nm and +1.8 x 10^{-3} at 530 nm for *r*-CP. For comparison, in the case of limonene-induced ***l*-PF8T2** particles,[16a] the magnitudes of g_{CPL} are –5.3 x 10^{-2} at 509 nm and –4.3 x 10^{-2} at 533 nm for **1*R***, while, +1.9 x 10^{-3} at 510 nm and +1.0 x 10^{-2} at 535 nm for (*S*)-limonene.

The absolute g_{CPL} values of these ***h*-PF8T2** particles, however, are rather weak by one-order of magnitude than those of the limonene-induced ***l*-PF8T2** particles,[16a] This means approximately 6−8 % optical purity relative to (*R*)-limonene-induced ***l*-PF8T2** particles. Limonene chirality is more efficient to induce optically active **PF8T2** particles with greater chiroptical amplitudes as well as the difference in the magnitude of g_{CD} values between limonene and CP-photon induced optically active **F8AZO** particles.[10n,16b]

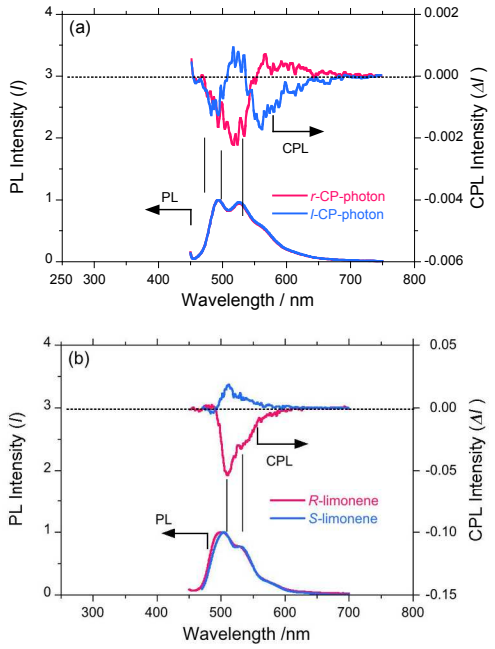

Fig. 7. A comparison of CPL spectra excited at 400 nm of (a) ***h*-PF8T2** particles induced by *r*- and *l*-CP-photon for 60 min in $CHCl_3$/MeOH (2.1/0.9 (v/v)) and (b) ***l*-PF8T2** particles produced by limonene chirality transfer in ((*R*)- and (*S*)-limonene)/$CHCl_3$/MeOH (2.0/0.3/0.7 (v/v)). CPL/PL data of Fig. 7b was taken from ref. 16a.

CP-photon irradiation successfully allowed us to produce CPL-active ***h*-PF8T2** particles (quantum yield (Φ_F) of 8 %) from the corresponding CPL-silent particles showing Φ_F of 15 %. The subtle decrease in Φ_F leads to an apparent weakening of the bright spots in the FOM image of ***h*-PF8T2** after the *r*-CP irradiation (Fig. 8). The decrease in Φ_F value after prolonged CP-photon irradiation may be ascribed to less efficient emissive thiophene sulfoxide, thiophene sulfone and fluorenone moieties that are air-oxidation products of thiophene rings and fluorenone of **PF8T2**.

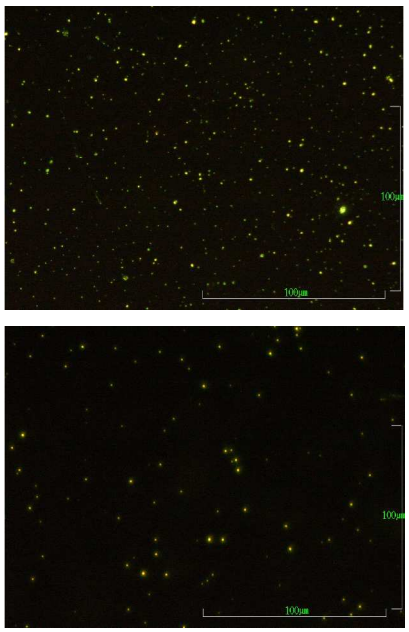

Fig. 8. Fluorescence optical images excited at 450-490 nm of ***h*-PF8T2** particle (top) before irradiating and (bottom) after *r*-CP-photon at 546 nm for 60 min. Scale bar: 100 μm.

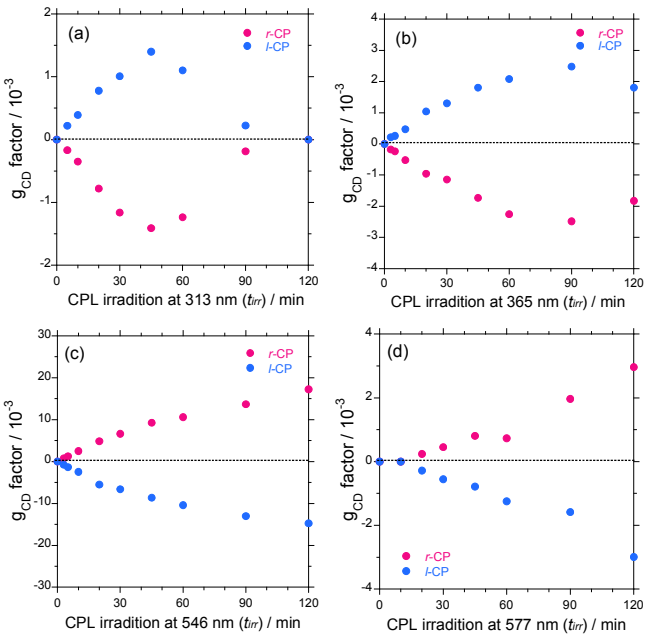

Fig. 9. The changes in g_{CD} values of ***h*-PF8T2** particles in $CHCl_3$/MeOH (2.1/0.9 (v/v)) as a function of irradiation time of *r*-photons (red filled circles) and *l*-CP-photons (blue filled circles) at (a) 3.96 eV (313nm), (b) 3.40 eV (365 nm), (c) 2.27 eV (546 nm) and (d) 2.15 eV (577 nm). Red and blue filled circles are *r*- and *l*-CP-photon, respectively.

Photodynamics monitored at 590–630 nm of ***h*-PF8T2** particles in $CHCl_3$/MeOH (2.1/0.9 (v/v)) generated by *r*-CP-photon at 546-nm was measured. The particles had τ_1 = 0.487 nsec (0.917) and τ_2 = 0.811 nsec (0.083) at room temperature,

as given Fig. S6 (ESI). The shorter τ_1 lifetime implies quantum coherence of cooperative emission process[18c] in the particles.

3.5 Chiroptical retention: Long-term chiroptical memory

The time-course change in chiroptical polarization ***h*-PF8T2** particles by *r*- and *l*-CP-photon in $CHCl_3$/MeOH (2.1/0.9 (v/v)) as a function of irradiation time at four energies (wavelengths), including 3.96 eV (313nm), 3.40 eV (365 nm), 2.27 eV (546 nm) and 2.15 eV (577 nm) are given in Figs. 9(a)–(d).

A prolonged *r*-CP-photon irradiation at 546 nm to **PF8T2** particles in the $CHCl_3$/MeOH cosolvents tends to gradually decrease M_n and to slightly increase polydispersity (M_w/M_n) values, regardless of higher and lower molecular mass (Fig. 10, Fig. S7 (ESI)). Main chain scission reaction, though not significant, may take place.

In the case of *r*-CP-photon irradiation at 313nm and 365 nm, the negative g_{CD} values progressively increase with irradiation time and decrease at 40–50 min at 313 nm irradiation and 90–100 min at 365 nm irradiation. Conversely, *l*-CP-photon irradiation at 313 nm and 365 nm provides the positive g_{CD} values progressively, obeying an almost mirror-image relationship (Figs. 9(a)–(b)).

r-CP-photon irradiation at 546 nm and 577 nm induces the positive g_{CD} values progressively with irradiation time up to 120 min. Conversely, *l*-CP-photon irradiation at 546 nm and 577 nm induces the negative g_{CD} values, obeying an almost mirror-image relationship (Figs. 9(c)–(c)). Notably, this chiroptical polarization induced by CP-photon irradiation is thermally stable when the particles were kept in suspension in the dark, as shown in Fig. 11(a). Also, this chiroptical polarization is thermally stable in the range of 15°C and 45°C upon heating-and-cooling runs, when the particles were kept in suspension, as shown in Fig. 11(b).

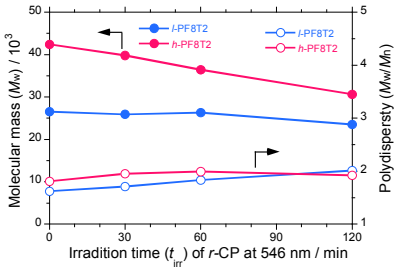

Fig. 10. The changes in molecular mass (M_n) and polydispersity (M_w/M_n) of **PF8T2** particles as a function of irradiation time of *r*-CP-photons at 2.27 eV (546 nm): ***h*-PF8T2** in $CHCl_3$/MeOH (2.1/0.9 (v/v)) and ***l*-PF8T2** in $CHCl_3$/MeOH (1.8/1.2 (v/v)).

3.6 Chiroptical depolarisation, inversion and switching

Based on the knowledge of chiroptical polarisation and long-term thermal retention, we succeeded in chiroptical restoration, inversion and switching to ***h*-PF8T2** particles in $CHCl_3$/MeOH (2.1/0.9 (v/v)) generated by *r*-CP-photon at 2.27 eV (546 nm), followed by alternating irradiation of *l- and r*-CP-photon at 2.27 eV (546 nm). As shown in Fig. 12 and Fig. S8 (ESI), it is evident that CD and UV-visible spectra of ***h*-PF8T2** particles in $CHCl_3$/MeOH (2.1/0.9 (v/v)) change in response to alternation in handedness of CP-photon at 2.27 eV (546 nm) with *r-l-l-r-r-l-l* for 30 min interval and *r-l-l-r-r* for 60 min interval cycles, respectively.

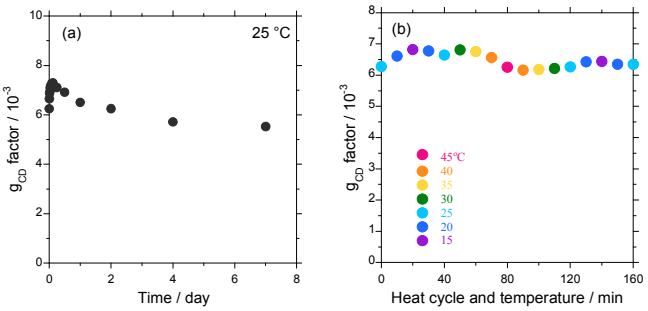

Fig. 11. (a) The chiroptical stability of chiroptically polarized ***h*-PF8T2** particles in $CHCl_3$/MeOH (2.1/0.9 (v/v)) at 25 °C as a function of time. (b) The chiroptical stability between 15 °C and 45°C of ***h*-PF8T2** particles in $CHCl_3$/MeOH (2.1/0.9 (v/v)). The particles obtained by irradiating *r*-CP-photon at 2.27 eV (546 nm) for 60 min were placed in the dark under controlled temperature.

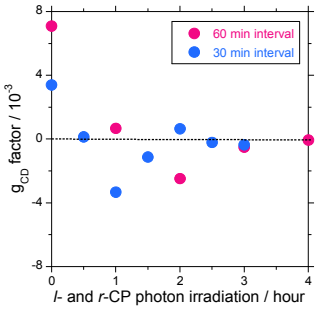

Fig. 12. The chiroptical depolarization, inversion and switching characteristics at 25 °C of ***h*-PF8T2** particles in $CHCl_3$/MeOH (2.1/0.9 (v/v)). The particles obtained by irradiating *r*-CP-photon at 2.27 eV (546 nm) for 30 min interval (blue filled circles) and for 60 min (red filled circles).

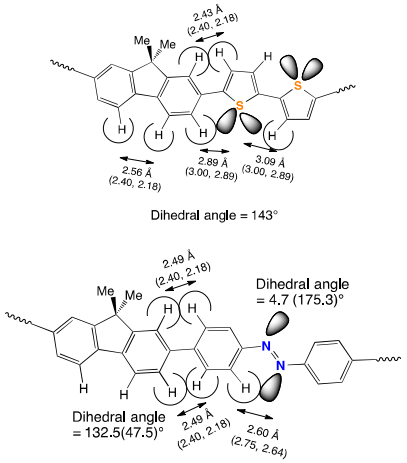

Fig. 13. (Left) H···H and H···S distances with van der Waals contacts (parenthesis) of ***oligo*-F1T2** with dihedral angle of 143° optimised with PM3. (Right) H···H and H···N distances with van der Waals contacts (parenthesis) of ***oligo*-F1AZO** with dihedral angle of 143° optimised with PM3.

Fig. 12 plots the change in g_{CD} values in response to the alternation of the CP-photon's handedness at 2.27 eV (546 nm) with *r-l-l-r-r-l-l* for 30 min and *r-l-l-r-r* for 60 min interval

cycles, respectively. It is evident that chiroptical restoration, inversion and switching are possible by the alternation of CP-photon's handedness. However, it is worth noting that upon CP-photon irradiation, the isosbestic point at ≈ 505 nm in the UV-visible and CD spectra can be seen (Fig. S8 (ESI). Certain re-organization in main-chain conformation takes place within the particles. Switching ability tends to weaken with repeating *r*-/*l*-CP cycles.

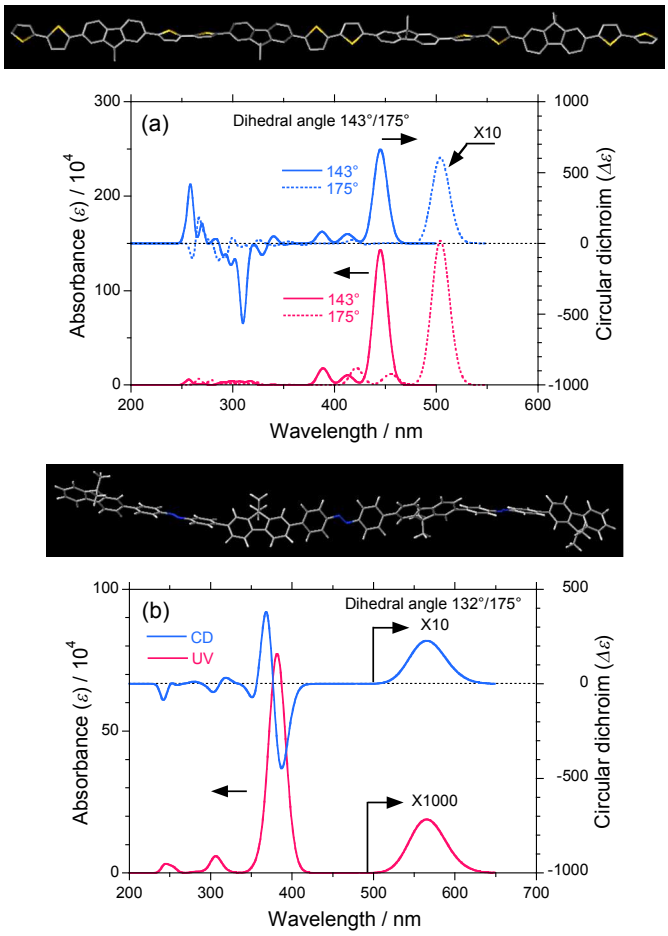

Fig. 14. (a) Simulated UV-visible and CD spectra (with a full-width-at-half-maximum (*fwhm*) = 0.05 eV, forty transition states) of helical ***oligo*-F1T2** with dihedral angles of 143° and 175°, obtained with semiempirical ZINDO based on optimisation of ***oligo*-F1T2** using molecular mechanics, MM (UFF), followed by PM3 calculation. Solid and dotted lines are ***oligo*-F1T2** with a dihedral angle of 143° and 175°, respectively. (b) Simulated UV-visible and CD spectra (with *fwhm* = 0.10 eV, forty transition states) of helical ***oligo*-F1AZO** with dihedral angles of 132.5° (47.5°) and 175.3° (4.7°), obtained with ZINDO calculation of ***oligo*-F1AZO** optimised with PM3 calculation.

3.7 A proposed mechanism for CP-photon energy dependence of chiroptical polarization to PF8T2 particles

The origin of CP-photon energy dependent chiroptical polarization is ascribed to the sign inversion of CD spectrum at shorter and longer wavelengths (higher and lower π–π* transition modes) of **PF8T2** itself. PM3 calculation of two hypothetical ***oligo*-F1T2** models with dihedral angles (the most stable by MM calculation) and 178° (unstable, but an almost coplanar geometry) an oligomeric model of **PF8T2**, suggested that the most energetically stable structure prefers a helical conformation twisted 143° with *P*-screw sense, even if an initial structure is generated initially from coplanar structure with all-trans conformation. The inherent twisting ability of ***oligo*-F1T2** and **PF8T2** derives from C-H···H-C and C-H···S repulsions of van der Waals contact between fluorene and thiophene rings, as illustrated in Fig. 13.

Other hypothetical helical ***oligo*-F1T2** models with dihedral angles of 120°, 143°, 160°, 175° and 178° showed a tendency for CD bands arising from intense π–π* absorption bands (main-chain parallel component with *P*-screw sense)[23] in the range of 350−500 nm to show positive sign, while several CD bands located at weak π–π* absorption bands (main-chain perpendicular components with *M*-screw sense) or *vice versa*[23] in the range of 280−350 nm had negative sign (ESI, Fig. S9). As dihedral angles decrease from 178° to 120°, λ_{max} values at the intense π–π* bands shift to shorter wavelengths (higher energies) due to a loss of effective π-conjugated length parallel to the main chain with *P*-screw sense, while λ_{max} values at the weak π–π* bands with *M*-screw sense remain almost unchanged due to the main chain perpendicular components.

Similarly, the most probable helical ***oligo*-F1AZO** model (dihedral angles, 132° (fluorene-phenylazo moieties) and 175° (azobenzene moiety)) optimised with MM calculation have positive-sign CD bands at weak n–π* band in the range of 500–620 nm, conversely, exhibit negative-sign weak CD bands associated with weak UV π–π* transition in the range of 300–350 nm (Fig. 14(b)).

The ZINDO calculation results thus suggest that swapping of chiroptical signs by the same *l*- and *r*-CP-photons is strongly connected to the swapping of chiroptical signs in shorter and longer wavelengths (or higher and lower photon energy) within **PF8T2** particles, and possibly, **PF8AZO** particles. Shorter wavelength (or higher photon energy) and lower wavelength (or lower photon energy) are capable to orthogonally excite the π–π* transitions that are main-chain perpendicular and parallel components, respectively. For example, when *l*-CP-photon excites main-chain parallel component, right-twisted helical motif is induced, conversely, when *l*-CP-photon excites main-chain perpendicular component, left-twisted helical motif is generated.

These computational results led us to a novel idea that, compared to single *r*- (or *l*-) CP-photon source, all chiroptical polarisation, depolarisation, inversion, retention and switching modes are more easily and efficiently controllable when two CP-photon sources with different irradiation energies (*fiat duo lux!*) are utilised, *e.g.*, to accelerate chiroptical polarisation using *r*-CP at 313/365 nm and *l*-CP at 546/577 nm and to decelerate chiroptical polarisation, followed by acceleration of chiroptical inversion using *r*-CP at 313/365 nm and *r*-CP at 546/577 nm.

3.8 Perspectives of optofluidically enhanced CP-photon chirality transfer to non-photochromic polymer particles

Controlled photon chirality transfer operated in optofluidic systems may provide a possible answer to a coacervate

hypothesis proposed by Oparin.[24] The hypothesis is that μm-order droplets of assorted organic molecules dispersed in aqueous conditions resemble an environment for the evolution of living cells. The hypothesis is nowadays abandoned because of the effects due to energetically *closed* system. Because all chiroptical polarisation, depolarisation, inversion, switching and retention modes within the polymer particles in the ground and photoexcited states is efficiently possible with the help of sense and irradiation energy, optofluidic systems comprising μm-sized polymer particles in *open system* by continuously flowing external CP-photon source efficiently lead to chiral organization as dissipative structure,[15] which can maintain photogenerated structures in the dark for a long time.

Recently, gigantic enhancement in CD, CPL, CDS and VCD signals of colloidal particles is one of the hottest issues.[5j,10n,16,17h,17i,18,25] The present knowledge sheds light on a more efficient design to attain CD $g_{CD} = \pm 2$ and $g_{CPL} = \pm 2$ induced by CP-photon sources only in the future.

Conclusion

In summary, we demonstrated for the first time CP-photon energy dependent chiroptical μm-sized **PF8T2** particles dispersed in optofluidically tuned $CHCl_3$-MeOH cosolvents. Our experimental and theoretical results elucidated that (i) the choice of higher- and lower-CP-photon energies and their handedness leads to inversion of CD spectra of **PF8T2**, (ii) either *l*- or *r*- CP-photon efficiently induces all chiroptical polarization, depolarization, inversion, a long-term retention (at least, seven days at 25 °C) and switching modes into achiral **PF8T2** particles, (iii) the CP-photon induced CD signals are resonantly accelerated at a specific n_D value of the cosolvents due to the optofluidic effect and (iv) molecular mass of **PF8T2** considerably affects these CD, ORD and UV-visible spectral characteristics. From ZINDO calculations, these characteristics should originate from the inherent nature that optically active polymers have the opposite sign CD bands in the higher and lower transition region, leading the opposite twisting ability regardless of CP handedness during irradiation. The present results shed light on a simple and efficient production of optically active particles assorted with polymeric species by two designed *r*- and/or *l*-CP-photons in different energies.

Acknowledgements

Financial support was provided by the Projects of the Grant-in-Aids from JSPS KAKENHI (23651092, 26620155, 22350052). WZ is grateful for the financial support from the National Nature Science Foundation of China (21104052, 21374072). NS thanks funding from a JSPS research fellowship for young scientists. MF thanks Nor Azura Abdul Rahim (Universiti Malaysia Perlis and NAIST), Yoshihito Nishioka (NAIST) and Takashi Matsuda (NAIST) for fruitful discussion of CPL, CD spectroscopy and optical microscope. We thank technical staffs of NAIST (Fumio Asanoma, Yasuo Okajima, Syouhei Katao and Masahiro Fujihara) for helps of solid-state ^{13}C-NMR spectra, WAXS, PL dynamics and differential scanning calorimetry of **PF8T2** samples. We are thankful to Leigh McDowell (NAIST) for English proofreading our manuscript.

Notes and references

[a] *Graduate School of Materials Science, Nara Institute of Science and Technology, 8916-5 Takayama, Ikoma, Nara 630-0036, Japan. E-mail: fujikim@ms.naist.jp*

[b] *Jiangsu Key Laboratory of Advanced Functional Polymer Design and Application, Department of Polymer Science and Engineering, College of Chemistry, Chemical Engineering and Materials Science, Soochow University, Suzhou Industrial Park, Suzhou 215123, China. E-mail: weizhang@suda.edu.cn*

† Electronic Supplementary Information (ESI) available: Power intensity of unpolarised and *r*-/*l*-CP light, WAXS data of ***h*-PF8T2**, DLS data of ***h*-PF8T2** particles before and after *r*-CP light at 546 nm, the CD and UV-visible spectra of **PF8T2** dissolved in dilute $CHCl_3$ after *r- and l*-CP light at 546 nm, changes in CD and UV-visible spectra of ***h*-PF8T2** particles in $CHCl_3$/MeOH irradiated by *r*- and *l*-CP-photon at six photon energies, HRTEM images of ***h*-PF8T2** particles before and after irradiation of *r*-CP-photon at 546 nm for 60 min, change in GPC charts of ***h*-** and ***l*-PF8T2** particles in $CHCl_3$/MeOH as a function of *r*-CP-photon irradiation at 436 and 546 nm, changes in CD and UV-visible spectra of ***h*-PF8T2** particles in $CHCl_3$/MeOH irradiated by alternating *r*- and *l*-CP-photon at 2.27 eV (546 nm), CD and UV-visible spectra of ***oligo*-F1T2** with six dihedral angles (120°, 143°, 160°, 175° and 178°) simulated with ZINDO programme and PL photodynamics of ***h*-PF8T2** particles. See DOI: 10.1039/b000000x/

1. (*a*) G. N. Lewis, *Nature*, 1926, **118**, 874; (*b)* http://www.aps.org/publications/apsnews/201212/physicshistory.cfm; This Month in Physics History. December 18, 1926: Gilbert Lewis coins "photon" in letter to *Nature*.
2. (*a*) R. A. Beth, *Phys. Rev.*, 1936, **50**, 115; (*b*) G. Grynberg, A. Aspect and C. Fabre, *Introduction to Quantum Optics: From the Semi-classical Approach to Quantized Light*, Cambridge Univ. Press (Cambridge, UK, 2010).
3. (*a*) L. Allen, M. W. Beijersbergen, R. J. C. Spreeuw and J. P. Woerdman, *Phys. Rev. A*, 1992, **45**, 8185; (*b*) N. B. Simpson, K. Dholakia, L. Allen and M. J. Padgett, *Opt. Lett.*, 1997, **22**, 52; (*c*) E. Brasselet, N. Murazawa, H. Misawa and S. Juodkazis, *Phys. Rev. Lett.*, 2009, **103**, 103903; (*d*) M. Padgett, J. Courtial and L. Allen, *Phys. Today*, 2004 (May), 35; (*e*) J. P. Torres and L. Torner (eds), *Twisted Photons: Applications of Light with Orbital Angular Momentum*, Wiley-VCH (2011).
4. For reviews and a book, see. (*a*) B. L. Feringa and R. A. van Delden, *Angew. Chem. Int. Ed.*, 1999, **38**, 3418; (*b*) Y. Inoue, *Chem. Rev.*, 1992, **92**, 741; (*c*) Y. Inoue and V. Ramamurthy, *Chiral Photochemistry: Molecular and Supramolecular Photochemistry*, CRC Press: Tokyo 2004.
5. (*a*) N. Berova, P. L. Polpvarapu, K. Nakanishi and R. W. Woody (Eds), *Comprehensive Chiroptical Spectroscopy*, Wiley, 2012); (*b*) H. P. J. M. Dekkers, in *Circular Dichroism: Principles and Applications*, 2nd Edition, N. Berova, K. Nakanishi and R. W. Woody (eds), Chapter 7, Wiley-VCH: New York (NY), 2000; (*c*) J. Crassous, A. Amon and J. Crassous, *Phys. Rev.* A, 2012, **85**, 023806.
6. (*a*) F. S. Kipping and W. J. Pope, *J. Chem. Soc. Trans.*, 1989, **73**, 606; (*b*) M. Sakamoto, *Chem. Eur. J.*, 1997, **3**, 684; (*c*) F. Toda, *Acc. Chem. Res.*, 1995, **28**, 480.
7. (*a*) O. Ohno, Y. Kaizu and H. Kobayashi, *J. Chem. Phys.*, 1993, **99**, 4128; (*b*) D. K. Kondepudi, J. Laudadio and K. Asakura, *J. Am.*

Chem. Soc., 1999, **121**, 1448; (*c*) J. M. Ribó, J. Crusats, F. Sagués, J. Claret and R. Rubires, *Science,* 2001, **292**, 2063; (*d*) A. Tsuda, M. A. Alam, T. Harada, T. Yamaguchi, N, Ishii and T. Aida, *Angew. Chem. Int. Ed.*, 2007, **46**, 8198; (*e*) M. Wolffs, S. J. George, Z. Tomović, S. C. J. Meskers, A. P. H. J. Schenning and E. W. Meijer, *Angew. Chem. Int. Ed*., 2007, **46**, 8203; (*f*) K. Okano, M. Taguchi, M. Fujiki and T. Yamashita, *Angew. Chem. Int. Ed*., 2011, **50**, 12474.

8. (*a*) G. L. J. A. Rikken and E. Raupach, *Nature*, 2000, **405**, 932; (*b*) Y. Xu, G. Yang, H. Xia, G. Zou, Q. Zhang and J. Gao, *Nat. Commun*., 2014, **5**, 5050.
9. (*a*) R. A. Rosenberg, *Top. Curr. Chem.*, 2011, **298**, 279; (*b*) J. M. Dreiling and T. J. Gay, *Phys. Rev. Lett*., 2014, **113**, 118103.
10. (*a*) K. L. Stevenson and J. F. Verdieck, *J. Am. Chem. Soc.*, 1968, **90**, 2974; (b) A. Moradpour, J. F. Nicoud, G. Balavoine, H. Kagan and G. Tsoucaris, *J. Am. Chem. Soc*., 1971, **93**, 2353; (*c*) W. J. Bernstein, M. Calvin and O. Buchardt, *J. Am. Chem. Soc*., 1972, **94**, 494; (*d*) Y. Zhang and G. B. Schuster, *J. Org. Chem*., 1995, **60**, 7192; (*e*) N. P. M. Huck, W. F. Jager, B. de Lange and B. L. Feringa, *Science*, 1996, **273**, 1686; (*f*) L. Nikolova, T. Todorov, M. Ivanove, F. Andruzzi, S. Hvilsted and P. S. Ramanujam, *Opt. Mater*., 1997, **8**, 255; (*g*) G. Iftime, F. L. Labarthet, A. Natansohn and P. Rochon, *J. Am. Chem. Soc*., 2000, **122**, 12646; (*h*) C. A. Khatri, Y. Pavlova, M. M. Green and H. Morawetz, *J. Am. Chem. Soc.*, 1997, **119**, 6991; (*i*) T. Kawasaki, M. Sato, S. Ishiguro, T. Saito, Y. Morishita, I. Sato, H. Nishino, Y. Inoue and K. Soai, *J. Am. Chem. Soc*., 2005, **127**, 3274; (*j*) S. W. Choi, T. Izumi, Y. Hoshino, Y. Takanishi, K. Ishikawa, J. Watanabe and H. Takezoe, *Angew. Chem. Int. Ed.*, 2006, **45**, 1382; (*k*) F. Vera, R. M. Tejedor, P. Romero, J. Barberá, M. B. Ros, J. L. Serrano and T. Sierra, *Angew. Chem. Int. Ed*., 2007, **46**, 1873; (*l*) J. Barberá, L. Giorgini, F. Paris, E. Salatelli, R. M. Tejedor and L. Angiolini, *Chem. Eur. J.*, 2008, **14**, 11209; (*m*) P. K. Hashim, R. Thomas and N. Tamaoki, *Chem. Eur. J.,* 2011, **17**, 7304; (*n*) M. Fujiki, K. Yoshida, N. Suzuki, J. Zhang, W. Zhang and X. Zhu, *RSC Adv.*, 2013, **3**, 5213; (*o*) K. Rijeesh, P. K. Hashim, S.-i. Noroa and N. Tamaoki, *Chem. Sci.*, 2015 (DOI: 10.1039/C4SC01993H).
11. (*a*) T. L. V. Ulbricht and F. Vester, *Tetrahedron*, 1962, **18**, 629; (*b*) S. F. Mason, *Nature*, 1984, **311**, 19; (*c*) L. D. Barron, *Chem. Soc. Rev*., 1986, **15**, 189; (*d*) M. Quack, *Angew. Chem. Int. Ed.*, 1989, **28**, 571; (*e*) R. A. Hegstrom and D. K. Kondepudi, *Sci. Am*., 1990, **262**, 98; (*f*) A. Salam, *J. Mol. Evol.*, 1991, **33**, 105; (*g*) V. Avetisov and V. Goldanskii, *Proc. Natl. Acad. Sci. USA*, 1996, **93**, 11435; (*h*) M. Avalos, R. Babiano, P. Cintas, J. L. Jiménez and J. C. Palacios, *Chem. Rev.*, 1998, **98**, 2391; (*i*) P. Schwerdtfeger, J. Gierlich and T. Bollwein, *Angew. Chem. Int. Ed*, 2003, **42**, 1293; (*j*) Y. Scolnik, I. Portnaya, U. Cogan, S. Tal, R. Haimovitz, M. Fridkin, A. C. Elitzur, D. W. Deamer and M. Shinitzky, *Phys. Chem. Chem. Phys*., 2006, **8**, 333; (*k*) E. K. Kodona, C. Alexopoulos, E. Panou-Pomonis and P. J. Pomonis, *J Colloid Interface Sci*., 2008 **319**, 72; (*l*) M. Fujiki, *Symmetry*, 2010, **2**, 1625.
12. (*a*) Y. J. Zhang, T. Oka, R. Suzuki, J. T. Ye and Y. Iwasa, *Science*, 2014, **344**, 725; (*b*) C. Pfeiffer, C. Zhang, V. Ray, L. J. Guo and A. Grbic, *Phys. Rev. Lett.*, 2014, **113**, 023902.
13. (*a*) J. Bailey, A. Chrysotomou, J. H. Hough, T. M. Gledhill, A. McCall, S. Clark, F. Ménard and M. Tamura, *Science*, 1998, **281**, 672; (*b*) D. B. Cline, *Eur. Rev.*, 2005, **13**, 49; (*c*) T. Fukue, M. Tamura, R. Kandori, N. Kusakabe, J. H. Hough, J. Bailey, D. C. B. Whittet, P. W. Lucas, Y. Nakajima and J. Hashimoto, *Orig. Life Evol. Biosph*., 2010, **40**, 335; (*d*) C. Meinert, S. V. Hoffmann, P. Cassam-Chenaï, A. C. Evans, C. Giri, L. Nahon and U. J. Meierhenrich, *Angew. Chem. Int. Ed.*, 2014, **53**, 210.
14. (*a*) T. Manaka, H. Kon, Y. Ohshima, G. Zou and M. Iwamoto, *Chem. Lett*., 2006, **35**, 1028; (*b*) Y. Wang, T. Sakamoto and T. Nakano, *Chem. Commun.*, 2012, **48**, 1871; (*c*) T. Nakano, *Chem. Rec.*, 2014, **14**, 369; (*d*) M. Miyata, M. Teraguchi, H. Endo, T. Kaneko and T. Aoki, *Chem. Lett*., 2014, **43**, 1476; (*e*) S.-T. Wu, Z.-W. Cai, Q.-Y. Ye, C.-H. Weng, X.-H. Huang, X.-L. Hu, C.-C. Huang and N.-F. Zhuang, *Angew. Chem. Int. Ed.*, 2014, **53**, 12860.
15. (*a*) I. Prigogine, G. Nicolis and A. Babloyants, *Phys. Today*, 1972 (Nov), 23; (*b*) I. Prigogine, G. Nicolis and A. Babloyants, *Phys. Today*, 1972 (Dec), 38; (*c*) R. Plasson, D. K. Kondepudi, H. Bersini, A. Commeyras and K. Asakura, *Chirality*, 2007, **19**, 589; (*d*) J. Zhou, J. Dong, B. Wang, T. Koschny, M. Kafesaki and C. M. Soukoulis, *Phys. Rev. B*, 2009, **79**, 121104.
16. (*a*) Y. Kawagoe, M. Fujiki and Y. Nakano, *New J. Chem.*, 2010, **34**, 637; (*b*) W. Zhang, K. Yoshida, M. Fujiki and X. Zhu, *Macromolecules*, 2011, **44**, 5105.
17. (*a*) D. Psaltis, S. R. Quake and C. Yang, *Nature*, 2006, **442**, 381; (*b*) C. Monat, P. Domachuk and B. J. Eggleton, *Nat. Photonics*, 2006, **1**, 106; (*c*) J. A. Sherwin and A. Lakhtakia, *Opt. Commun.*, 2002, **214**, 231; (*d*) J. Pedersen and N. A. Mortensen, *Appl. Phys. Lett.*, 2007, **91**, 213501; (*e*) N. A. Mortensen and S. Xiao, *Appl. Phys. Lett*., 2007, **90**, 141108; (*f*) F. B. Arango, M. B. Christiansen, M. Gersborg-Hansen and A. Kristensen, *Appl. Phys. Lett.*, 2007, **91**, 223503; (*g*) H. C. Hunt and J. S. Wilkinson, *Microfluid. Nanofluid.*, 2008, **4**, 53; (*h*) Y. Nakano and M. Fujiki, *Macromolecules*, 2011, **48**, 7511; (*i*) M. Fujiki, A. J. Jalilah, N. Suzuki, M. Taguchi, W. Zhang, M. M. Abdellatif and K. Nomura, *RSC Adv.* 2012, **2**, 6663.
18. (*a*) A. Ghosh and P. Fischer, *Phys. Rev. Lett.*, 2006, **97**, 173002; (*b*) M. P. Silverman, J. Badoz and B. Briat, *Opt. Lett.*, 1992, **17**, 886; (*c*) M. P. Silverman, *Quantum Superposition. Counterintuitive Consequences of Coherence, Entanglement, and Interference*, Springer: Berlin, 2007.
19. (*a*) R. F. Rodrigues, A. Charas, J. Morgado and A. Maçanita, *Macromolecules*, 2010, **43**, 765; (*b*) L. Huang, L. Zhang, X. Huang, T. Li, B. Liu and D. Lu, *J. Phys. Chem. B*, 2010, **118**, 791.
20. (*a*) M. Kasha, *Radiation Res*., 1963, **20**, 55; (*b*) M. Kasha, R. Rawls and M. S. El-Bayoumi, *Pure Appl. Chem.*, 1965, **11**, 371.
21. M. J. Frisch, G. W. Trucks, H. B. Schlegel, G. E. Scuseria, M. A. Robb, J. R. Cheeseman Jr., J. A. Montgomery, T. Vreven, K. N. Kudin, J. C. Burant, J. M. Millam, S. S. Iyengar, J. Tomasi, V. Barone, B. Mennucci, M. Cossi, G. Scalmani, N. Rega, G. A. Petersson, H. Nakatsuji, M. Hada, M. Ehara, K. Toyota, R. Fukuda, J. Hasegawa, M. Ishida, T. Nakajima, Y. Honda, O. Kitao, H. Nakai, M. Klene, X. Li, J. E. Knox, H. P. Hratchian, J. B. Cross, V. Bakken, C. Adamo, J. Jaramillo, R. Gomperts, R. E. Stratmann, O. Yazyev, A. J. Austin, R. Cammi, C. Pomelli, J. W. Ochterski, P. Y. Ayala, K. Morokuma, G. A. Voth, P. Salvador, J. J. Dannenberg, V. G. Zakrzewski, S. Dapprich, A. D. Daniels, M. C. Strain, O. Farkas, D. K. Malick, A. D. Rabuck, K. Raghavachari, J. B. Foresman, J. V. Ortiz, Q. Cui, A. G. Baboul, S. Clifford, J. Cioslowski, B. B. Stefanov, G. Liu, A. Liashenko, P. Piskorz, I. Komaromi, R. L. Martin, D. J. Fox, T. Keith, M. A. Al-Laham, C. Y. Peng, A. Nanayakkara, M. Challacombe, P. M. W. Gill, B. Johnson, W. Chen, M. W. Wong, C. Gonzalez and J. A. Pople, GAUSSIAN 03 (Rev. E.01), Gaussian, Inc., Wallingford CT, 2004.
22. G. C. Righini, Y. Dumeige, P. Féron, M. Ferrari, G. N. Conti, D. Ristic and S. Soria, *Riv Nuovo Cimento*, 2011, **34**, 435.
23. G. Snatzke, Chapter 1, Circular Dichroism: An Introduction, In *Circular Dichroism: Principle and Applications, 2nd Edition*, N. Berova, K. Nakanishi and R. W. Woody (eds), Wiley-VCH: New York (NY), 2000.
24. A. I. Oparin and V. G. Fesenkov, *Life in the Universe*, Twayne, Publishers, New York (NY), 1961.
25. (*a*) S. R. Domingos, A. Huerta-Viga, L. Baij, S. Amirjalayer, D. A. E. Dunnebier, A. J. C. Walters, M. Finger, L. A. Nafie, B. de Bruin, W. J. Buma and S. Woutersen, *J. Am. Chem. Soc.*, 2014, **136**, 3530; (*b*) K. Watanabe and K. Akagi, *Sci. Tech. Adv. Mater*., 2014, **15**, 44203. (*c*) J. Liu, H. Su, L. Meng, Y. Zhao, C. Deng, J. C. Y. Ng, P. Lu, M. Faisal, J. W. Y. Lam, X. Huang, H. Wu, K. S. Wong and B. Z. Tang, *Chem. Sci.* 2012, **3**, 2737; (*d*) X. Jiang, X. Liu, Y. Jiang, Y. Quan, Y. Cheng and C. Zhu, *Macromol. Chem. Phys*., 2014, **215**, 358; (*e*) M. Fujiki, Y. Kawagoe, Y. Nakano and A. Nakao, *Molecules*, 2013, **18**, 7035; (*f*) J. Liu, J. Zhang, S. Zhang, N. Suzuki, M. Fujiki, L. Wang, L. Li, W. Zhang, N. Zhou and X. Zhu, *Polym. Chem*., 2014, **5**, 784; (*g*) L. Wang, Nozomu Suzuki, J. Liu, T. Matsuda, N. A. A. Rahim, W. Zhang, M. Fujiki, Z. Zhang, N. Zhou and X. Zhu, *Polym. Chem.*, 2014, **5**, 5920; (*h*) M. Fujiki, *Symmetry*, 2014, **6**, 677 and references cited therein.

Graphical Abstract

Photon Magic: Chiroptical Polarisation, Depolarisation, Inversion, Retention and Switching of Non-photochromic Light-emitting Polymer in Optofluid

Michiya Fujiki,[*,a] Yuri Donguri,[a] Yin Zhao,[b] Ayako Nakao,[a] Nozomu Suzuki,[a] Kana Yoshida[a] and Wei Zhang[*,b]

[a] *Graduate School of Materials Science, Nara Institute of Science and Technology, 8916-5 Takayama, Ikoma, Nara 630-0036, Japan. E-mail: fujikim@ms.naist.jp*

[b] *Jiangsu Key Laboratory of Advanced Functional Polymer Design and Application, Department of Polymer Science and Engineering, College of Chemistry, Chemical Engineering and Materials Science, Soochow University, Suzhou Industrial Park, Suzhou 215123, China.*

Circularly polarized photon hand, *l*- and *r*-, was *not a deterministic factor for the induced chiroptical sign* of π-conjugated polymer aggregates. This anomaly originates from circular dichroism inversion characteristics between shorter and longer π–π* bands, supported by ZINDO calculation of the model oligomers.